SEMICONDUCTOR DETECTORS OF NUCLEAR RADIATION

E. L. STOLYAROVA

INTRODUCTION

SEMICONDUCTOR detectors, which were recently developed both here and abroad, are most suitable for the registration and spectroscopy of charged heavy particles (fission fragments, alpha particles, protons, etc.) and also for the registration and spectroscopy of neutrons.

Semiconductor spectrometers for heavy charged particles and neutrons, have many valuable properties. They have good resolution (several tenths of 1%), they withstand considerable currents (up to 10^{14} protons and 10^{11} alpha particles per square centimeter), and permit ready cutoff of the gamma background.

Semiconductor detectors are compact, cheap, simple to manufacture and use, and require no high-voltage power supplies.

In the present article we report on the physical principles, construction, and main parameters of semiconductor detectors for various nuclear radiations, and also the prospects of their utilization in various branches of nuclear physics.

1. Crystal Counters

The forerunners of semiconductor counters were crystal counters. The first crystal counter used to register individual nuclear particles was described by Van Heerden in 1945 (see [1]); he used silver chloride crystals for this purpose, and was able to register alpha and beta particles and gamma quanta. The pulses produced by such counters have a front rise time on the order of 2×10^{-7} sec and an amplitude reaching 1 mV. There are reports of mixed LiBr–AgB crystals[2] used for the registration of neutrons, using the reaction $Li^6(n, \alpha)He^3$. The neutron registration efficiency attained with crystals measuring 1.2×0.75 cm was 5%. The author believes that at a crystal thickness of 2 cm, using enriched Li^6, the neutron registration efficiency can be raised to 70%.

There are many descriptions of diamond counters [1], which are particularly interesting to physicians since (1) the electron density in diamond is close to that in living tissues and (2) it is possible to manufacture very small counters for internal research. The registration of nuclear radiation by single CdS crystals was described in [3,4] and elsewhere. It was found that there are two types of CdS crystals; the first gives short pulses ($t_{rise} = 10^{-7}-10^{-8}$ sec) of small amplitudes, while the second gives pulses of longer duration ($t_{rise} = 10^{-5}-10^{-3}$ sec) and an ampli-

tude 10^4 times larger (the so-called effect of internal amplification of the signal). This effect is completely eliminated by infrared radiation.

CdS crystals were used to register alpha particles from Po, beta particles from RaE, and gamma quanta from MsTh and Co^{60} [4].

The registration of particles by a crystal counter reduces to the registration of the voltage pulses which result from an increase in the crystal conductivity under the influence of the charged particles striking it.

Figure 1a shows a schematic diagram of a crystal counter, in which the charged particle, for example an alpha particle, produces electron-hole pairs. An external potential difference U is applied to the ends of the crystal through metallic plates A and B, and produces in the crystal an electric field $E \approx U/l$. The holes and the electrons move under the influence of the external field. This displacement is defined by

$$W = \mu E \tau,$$

where μ is the mobility, E the electric field, and τ the lifetime of the carriers. When the charge carriers (electrons and holes) move they induce a charge on the plates Q_i, proportional to the traversed potential difference:

$$Q_i = q \frac{\Delta U}{U}, \tag{1}$$

where q is the carrier charge and ΔU the potential difference traversed by the carriers (Fig. 1b).
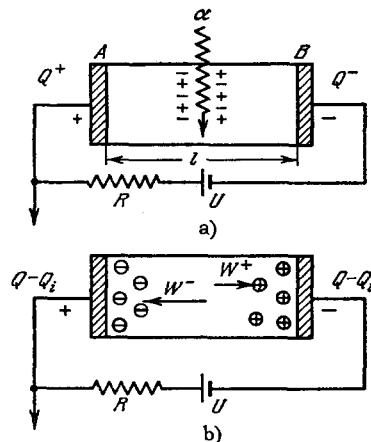

FIG. 1. a) Schematic diagram of crystal counter: U—applied voltage, R—resistor, Q^+ and Q^-—charges on plates A and B, α—charged particle producing pairs (electrons and holes); b) the motion of the carriers changes the charge produced on the plates by the external field.

When $W < l$, the carriers are captured inside the crystal and settle in traps (impurity centers, crystal defects), producing a space charge that creates in turn a field opposite to the external field. This is called the polarization effect. The polarization effect decreases the amplitude of the next signal. If the crystal counter operates for a long time in intense radiation fields, the average number of electrons and holes in the traps becomes so large that the amplitudes of the pulses decrease gradually until the counter stops operating altogether. To eliminate the polarization of the crystals, many authors have employed different means: infrared radiation, alternating electric field, alternation of counting and depolarization periods, activation with ultraviolet or beta rays, and thermal excitation[1,5].

2. Semiconductor Detectors

The shortcomings of crystal counters have stimulated a search for new ways and have led to the development of germanium and silicon counters. Their operating principle is similar to that of ionization chambers. The electric field is produced in a medium with low conductivity. When a charged particle penetrates this medium, collisions and ion-pair production occur in the case of a gas chamber, and electron-hole pairs are produced in the case of a solid chamber (semiconductor detector). In the ideal case the charges should be separated by the electric field and collected on boundaries, thus producing an electric pulse which can be amplified and recorded.

The requirements imposed on a good counter can be formulated as follows: the recombination of the charges prior to their collection should be eliminated, and therefore the medium must have high carrier mobility, must be free of defects, and must withstand high field gradients without breakdown.

1. PHYSICAL PRINCIPLES OF SEMICONDUCTOR DETECTORS FOR NUCLEAR RADIATION

The valence band of a dielectric or a semiconductor is filled even at absolute zero. In the conduction band, the electrons can move freely through the crystal under the action of an applied electric field. The valence and conduction bands are separated by the forbidden-energy band.

In real crystals there are defects due to displacements of the atoms, the presence of impurity atoms, etc., so that the electrons can have an energy which is forbidden in an ideal crystal. Consequently, the observed conductivity of dielectrics or semiconductors is determined essentially by the ionization of the impurity centers. Carriers of both polarities can participate in the conductivity, but as a rule the mobility of the electrons is much larger than that of the holes.

When a heavy charged particle, say an alpha par-

ticle, proton, etc., enters a semiconductor, it transfers its energy to the electrons by collision. The energy transferred by an alpha particle during each collision is not very large, owing to the large difference between the alpha-particle and electron masses, namely, the maximum energy which an electron can acquire is

$$E_{max} = 4 \frac{m}{M} E, \tag{2}$$

where m is the electron mass, M the alpha particle mass, and E the alpha particle energy.

Electrons that have acquired energy can move from the valence band into the conduction band; cases in which the electrons move from deeper levels filled by electrons into higher unfilled levels are also possible. This process is illustrated in Fig. 2a. As a result, electrons appear in bands which are normally not filled, and holes appear in those which are normally filled. This state can exist only for $\sim 10^{-12}$ sec, after which the interaction between the electrons and the holes causes the electrons to drop to the bottom of the lowest lying unfilled band, and the holes rise to the upper part of the highest filled band and are arranged as shown in Fig. 2b. Subsequently, owing to the removal of the excitation, a large number of Auger electrons is produced.*

In the mean, the energy consumed in this multi-step process in the production of one electron-hole pair, the so-called average ionization energy $\bar{\mathscr{E}}$, depends in
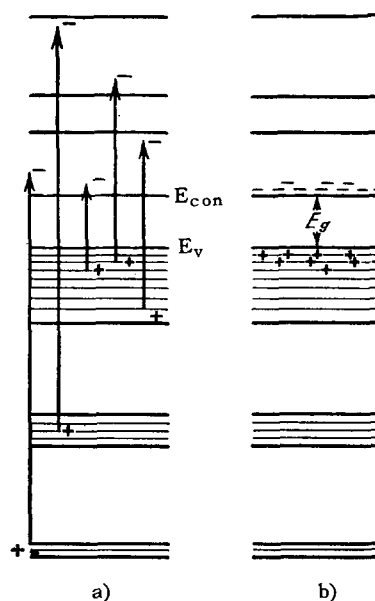

FIG. 2. a) Excitation of electrons in a semiconductor, due to the passage of a charged particle (alpha particle, proton, etc.); b) residual electron-hole excitation after 10^{-12} sec. E_{con}—voltage in the conduction band, E_v—in the valence band, E_g—in the gap between the bands.

*Low-energy electrons which leave the atomic levels as a result of the energy acquired when the excitation is removed.

practice, as shown by experiment, only on the material used to manufacture the semiconductor.

When the energy of the primary particle becomes smaller than the energy necessary for pair production, the main type of interaction is elastic scattering. The last step in the removal of the excitation is the recombination of the electrons and holes.

The mean free paths of the low-energy electrons are small, $\sim 1000 \text{Å}$ [9], so that the track of the primary particle is surrounded by a thin cylindrical layer of plasma made up of electrons and holes.*

If the primary charged particle is an electron, then the secondary electrons will have higher energies and larger ranges than in the case of heavy particles, since the equality of the primary and secondary particle masses causes the energy transfer to be appreciable. A cascade of electrons is produced with an energy spread which is larger than in the case of heavy particles, and the density of the electron-hole pairs will be considerably smaller.

The electrons and holes move as a result of the voltage applied to the counter, and an electric current is produced. The charge accumulated on the electrodes serves as a measure of the energy given up by the primary particle in the detector (Fig. 3a). The contribution made to this current by each carrier can be estimated in the following manner. Let e and v be the charge and velocity of the carrier, and E the local electric field; then the variation of the carrier energy in the field of the charge capacitor will be

$$evE = \frac{d}{dt}\left(\frac{Q^2}{2C}\right) = \frac{dQ}{dt}\frac{Q}{C} = iU,$$ (3)

where U and C are the total voltage on the capacitor and the capacitance. From (3) it follows that

$$i = \frac{evE}{U}.$$ (4)

Expression (4) can be rewritten in the form

$$i = e\frac{dx}{dt}\frac{1}{U}\frac{dU}{dx} = \frac{e}{U}\frac{dU}{dt},$$ (5)

where dU/dt is the rate of change of the potential due to the drift of the carriers in the electric field. Integrating (5) with respect to the time we obtain

$$\int i\,dt = Q_{\text{eff}} = \frac{e}{U}\Delta U.$$ (6)

Formula (6) gives the variation of the effective charge on the electrodes, due to the motion of one carrier of charge e in a field with potential difference ΔU, amounting to a definite fraction of the total capacitor voltage U. Equations (4)—(6) do not depend on the form of the field.

In the field of a parallel-plate capacitor the field intensity is

$$E = \frac{U}{d} = \text{const},$$

where d is the distance between the plates. Recognizing that the carrier velocity is

$$v = \mu E,$$ (7)

where μ is the carrier mobility, the contribution made by each carrier to the total current can be written in the form

$$i = \frac{e\mu E^2}{U} = \frac{e\mu U}{d^2}.$$ (8)

Figure 4b shows the waveform of the current produced as a result of the motion of a pair of carriers in the capacitor (Fig. 4a). The first pair (case 1) is produced near the negative electrode and the electron crosses the field; in the second case the active carrier is the hole, while in case 3 both the hole and the electron are active carriers.

The contributions to the current are determined from (8), and the duration of the current pulse is determined by the carrier drift time. The integral of the current with respect to the time is the same in all three cases and is equal to the electron charge.
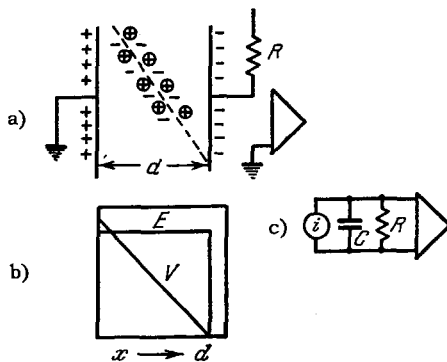
FIG. 3. a) Semiconductor ionization chamber with electron-hole pairs produced by a fast charged particle; b) potential and field distribution; c) equivalent circuit of the chamber with a current generator produced by the motion of the charged particles, holes, and electrons in the electric field.
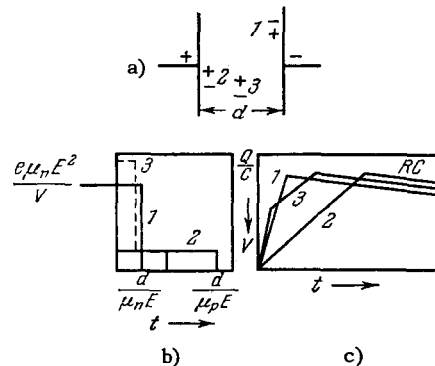
FIG. 4. a) Three electron-hole pairs produced in different places of the sensitive volume of a semiconductor chamber; b) current produced by each pair; c) voltage at the output of the amplifier of Fig. 3c, due to the current in Fig. 3b.

*With energy loss in Si of about 4 MeV/cm, the pair density in the plasma is $\approx 10^{16}$ cm^{-3}.

It is seen from Fig. 4 that in the case of simultaneous displacement of both carriers, the total charge transferred to the electron is equal to a single electron charge. In Fig. 3c is shown the equivalent circuit of a chamber with a current generator in place of a source of electrons and holes; C is the capacitor and R is the charging resistance.

The pulse rise time in a semiconductor is close in order of magnitude to the time of passage of the carrier through the counter, which in turn can be approximately estimated from the formula

$$t = \frac{d}{\mu E} .$$ (9)

As shown in [7], the carrier mobility does not remain constant in fields above 10^3 V/cm; this is also seen from Fig. 5. This can be attributed to the increase in the average carrier energy with the increasing electric field, and consequently to the decrease of their mean free path.
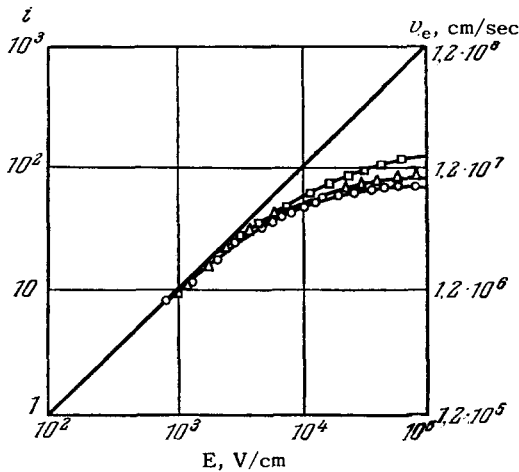

FIG. 5. Dependence of the electron velocity on the electric field, after Prior[1]. i—normalized current density, o—4.8, △—80, □—300 ohm-centimeters.

The presence of defects and impurities in the crystals, which leads to the formation of traps and recombination centers, can change the foregoing picture considerably. When an electron falls into a trap, it can be released after some time. However, a two-step process, which consists of the capture of an electron and hole, followed by their recombination, is also possible, and in this case the two carriers go out of play and the total current decreases.

When an electron is released from a trap it either returns to the valence band or continues its drift in the field towards the positive electrode. In the latter case this leads to an increase in the pulse rise time. The time that the electron stays in the trap is a function of the temperature. The processes of capture and recombination also depend on the temperature.

The recombination time (the time elapsed from the instant of production of the electrons and holes to their

recombination, or the lifetime τ_r) depends on the electron and hole capture cross section, the density of the capture centers N, and the electron thermal velocity v_t[9].

The recombination time is

$$\tau_r = \frac{1}{N \sigma v_t} .$$ (10)

In order for the passage of the electron through the counter to occur without considerable trapping, high purity of the material is necessary, with a low capture center concentration N; then $t \ll \tau_r$. Analogous arguments hold for holes.

To obtain a sufficiently large electric field in a semiconductor, it is important that its resistivity

$$\varrho = \frac{1}{n e \mu_n + p e \mu_p}$$ (11)

be sufficiently high. In an n-type semiconductor (for example, n-type Si) there are contaminations, donors, which have energy levels that are close to the edge of the conduction band[8].

At room temperatures, the electrons which are "ionized from the donors," are in the conduction band. At a donor concentration $N = 10^{13}$ cm^{-3}, the electron concentration in the conduction band will be close to

$$n = 10^{13} \text{ el/cm}^3$$

and the hole concentration will be very small, with the resistivity of the order of[9]

$$\varrho = 500 \ \Omega\text{-cm}$$

Acceptor impurities are fully analogous to donors, except that their levels are located adjacent to the valence band and they produce carriers of opposite sign[8].

Acceptors partially balance out the donors, and part of the donor electrons are captured by them in place of entering the conduction band. Thorough purification can decrease the concentration of the electrons and holes in silicon to the minimum possible value, 10^{10} carriers/cm^3 [9]. These carriers are called intrinsic. They are the results of the relatively improbable excitation of electrons via the forbidden energy band E_g = 1.1 eV. The product np of the electron and hole concentrations depends on the type of semiconductor and on the temperature, but does not depend on the concentration of the impurities. The concentration of the electrons or holes can be greatly modified by the impurities, but high concentration of the electrons is of necessity accompanied by low concentration of holes.

For Si at room temperature, np = 10^{20} electron-hole/cm^6, and the minimum total carrier concentration is obtained when n = p = 10^{10} electron/cm^3.

The temperature dependence is given by the expression

$$n_T p_T = n_0 p_0 \alpha e^{-\frac{E_g}{kT}},$$ (12)

where n_T and p_T are the concentrations of the elec-

trons and holes respectively at temperature T, E_g is the energy of the forbidden band in the semiconductor, and α is a proportionality coefficient. With decreasing temperature, the concentration of the conduction electrons decreases sharply. At 20°K it reaches n $= 10^5$ electrons/cm^3, and the resistivity is $\rho \approx 10^{10}$ ohm-cm[9]. This method of obtaining very high resistance is limited by the phenomenon of impact ionization, which is produced in electric fields exceeding 100 V/cm[10], and which leads to the formation of secondary electrons.

In [11] a method was proposed for combatting impact ionization, consisting of the use of such donor and acceptor impurities, as would have energy levels located sufficiently far within the intermediate band (far from the edges of both the conduction and valence bands). An example of such an impurity for Si is gold. Gold serves as an acceptor, capturing electrons from both the conduction band and from the donors. The limit to which the electron concentration can be reduced at room temperature is that of the intrinsic carrier, that is, 10^{10} electrons/cm^3; when the semiconductor is cooled to 78°K, the electron concentration can be reduced to 10^5 cm^{-3}. The electrons captured by the fold impurity are not released following collisions, since the ionization energy is high. Counters constructed on this principle have exhibited good operation[12,13].

Another way of obtaining a region with low carrier concentration in the semiconductor is to use a depletion layer in the p-n junction, the depth of which can be made sufficiently large by applying to the p-n junction an inverse bias voltage[6,15,18,19,26].

Figure 6a shows schematically the arrangement of the energy bands in the case of an equilibrium junction (without bias). In this case the junction is due to the diffusion of the donor impurities to a small depth into the initially highly purified p-type material. The layer on the surface is of the n-type with high electron concentration. The material on the inside is of the p-type with relatively low hole concentration.

The electrons have a tendency to diffuse to the right and the holes to the left, and this leads to the formation of a potential barrier for such a current. A space-charge region is produced artificially, made up on one side, of donors without a suitable number of electrons, and made up on the other side of acceptors without the corresponding number of holes (that is, a layer from which the carriers have been depleted). This region should contain an equal number of donors and acceptors of opposite signs, and since the concentration of the acceptors is much lower than that of the donors, the space-charge region is much broader on the p-side than on the n-side. The potential difference between the p and n sides reaches 0.5 V, and the width of the depletion layer is $\approx 10^{-3}$ cm.

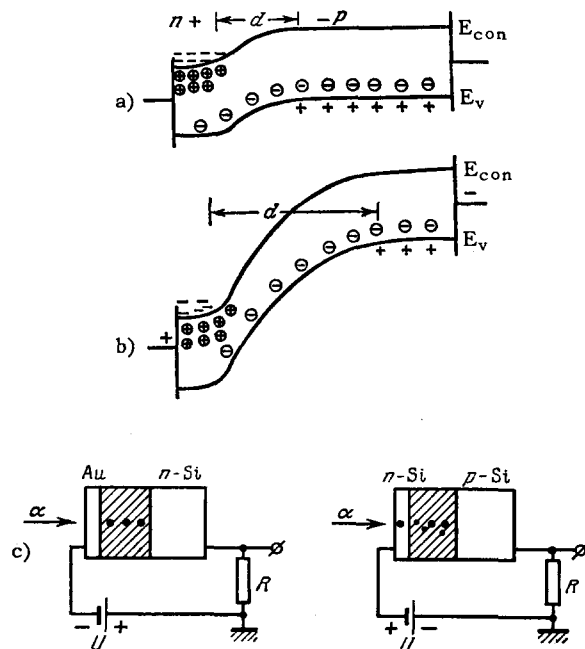A reverse bias broadens the depletion layer, producing a sufficiently sensitive effective volume for the

FIG. 6. a)Arrangement of the energy bands in equilibrium n-p junction; b) the same for a biased junction with bias voltage U; c) diagram of semiconductor counter.

detection of particles (Fig. 6b). An ionizing particle entering into the sensitive volume of the counter gives up its energy to the electrons by inelastic collision, and produces electron-hole pairs. In the mean, the energy consumed in the production of one pair, regardless of the type of radiation and its energy, is $\bar{\mathscr{E}}$ $= (2.94 \pm 0.15)$ eV in germanium and $\bar{\mathscr{E}} = (3.5 \pm 0.07)$ eV in silicon.

The capacitance C of the sensitive layer is also an important parameter, since its value governs the amplitude of the pulse. Knowing C, we can estimate the width of the depletion layer l, by representing C as a parallel-plane capacitor; then $l = \epsilon S/4\pi C$, where S is the area of the crystal and ϵ its dielectric constant. Since for the given counter $l \sim \sqrt{U_0 - U}$, we have

$$C \sim \frac{1}{\sqrt{U_0 - U}},$$

which agrees with experiment.

The pulse amplitude is proportional to the charge accumulated in the capacitor; since the charge is

$$Q = Ne = \frac{Ee}{\bar{\mathscr{E}}}, \quad \text{we get} \quad \Phi = \frac{Ee}{\bar{\mathscr{E}}(C + C_W)},$$

where N is the number of pairs produced by ionization, and $\bar{\mathscr{E}}$ is the average energy needed for the production of one pair.

The number N of pairs produced by ionization is proportional to the particle energy E.

By bombarding a counter with particles of one type but of different energy, for example α particles of different energy, and collecting the entire charge, we find that the pulse amplitude is linearly dependent on the α-particle energy (Fig. 7a).
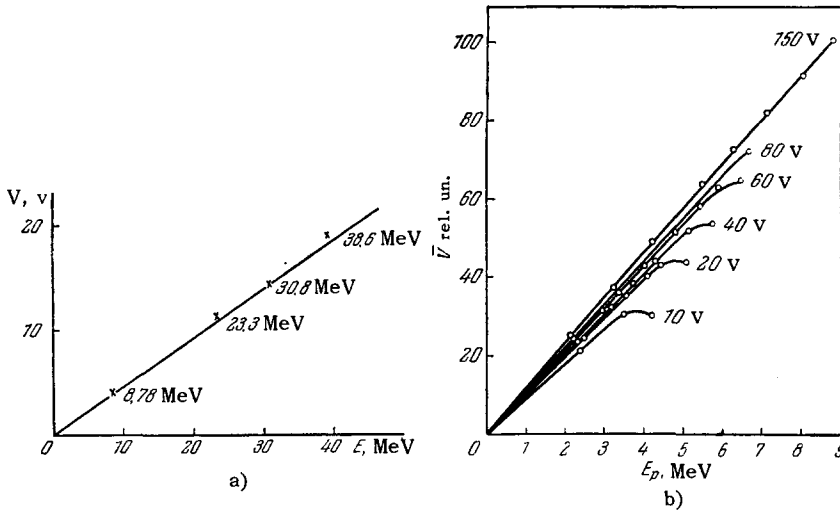
FIG. 7. a) Linearity of pulse amplitude with α-particle energy; b) signal amplitude V vs. proton energy E_p in MeV. The parameter is the bias voltage U in volts.

It is seen from the figure that the barrier depth (region of linearity of V vs. E_p) increases with increasing bias voltage U. The figure shows the values U = 10 and 2— V.

A large bias leads to a smaller capacitance, to a larger range of linear sensitivity, and a larger signal amplitude. If the charged particles have an energy that is so large that they leave the sensitive volume, the pulse amplitude decreases sharply. This is clearly seen in Fig. 7b.

These pairs are separated by the electric field of the space-charge layer (depletion layer), and the charge Q released by the ionization is collected by the total capacitance, consisting of the layer capacitance C and the wiring capacitance C_W. The capacitance is charged to a potential

$$\Phi = \frac{Q}{C + C_W} . \tag{13}$$

The voltage pulse picked off the load resistor R is registered by an electronic circuit. The ionizing particles usually arrive at the crystal perpendicular to the junction surface (Fig. 6c).

The pulse amplitude is linear in the energy of the ionizing particle and the amplitude resolution is good when the entire range of the particle lies inside the depletion layer l. The width of the depletion layer l can be represented in the form [15]

$$l = k \sqrt{\varepsilon(U_0 - U)\varrho\mu} \tag{14}$$

where ε is the dielectric constant of the semiconductor, U_0 the contact potential difference of the n and p regions in volts, U the reverse voltage (bias) in volts, ρ the resistivity of the silicon or germanium in ohm-cm, and μ the carrier mobility.

It is seen from the last formula that in order to obtain good n-p junction parameters it is important to have as high a resistivity ρ of the initial crystal as possible, and a sufficiently large bias voltage U.

In the general case when particles pass through the counter, the carriers will be produced both within the depletion layer and outside the layer. Accordingly, the resultant voltage pulses will have two components— fast and slow, produced by electron-hole pairs gener-

ated inside and outside the depletion layer, respectively [16].

The time characteristics of the semiconductor counters are determined by the carrier mobility. The electron mobility in silicon at room temperature is μ_n = 1300 cm^2/V-sec; the hole mobility is one-third as large, μ_p = ~ 430 cm^2/V-sec. For a specified barrier depth and bias, the time necessary to accumulate the charge can be calculated. In the first approximation we neglect the time necessary to separate the electrons and the holes, that is, the time during which the carriers diffuse before the collecting field overcomes their mutual attraction. The rise times of the voltage pulses, calculated in first approximation, range between 10^{-8} and 10^{-9} sec. Experiment has yielded for the rise time of pulses from off particles with energy E_α = 5 MeV at a barrier depth l = 120μ in a gold-silicon surface-barrier counter, with a bias U = 72 V and a resistivity ρ = 1000 ohm-cm, a value t_{exp} = 6 × 10^{-9} sec. The rise time calculated for this case is

$$t_{calc} = 3 \cdot 10^{-9} \text{ sec.}$$

Since the electron mobility in germanium is even higher,

$$\mu_{e\,Ge} = 1.5 \cdot 10^4 \text{ } cm^2/V\text{-sec.}$$

the rise time of the pulse in a germanium counter is even smaller than in a silicon counter

$$t_{rise} = 5 \cdot 10^{-10} \text{ sec.}$$

With such a steep pulse front for the fast component, the pulse rise time is usually limited to a considerable degree by the capabilities of the electronic circuit rather than the detector response. The decay of the pulse is determined by the time constant RC of the electronic circuit and is regulated by the value of the load resistance.

2. TECHNOLOGY OF MANUFACTURE OF SEMICON- DUCTOR COUNTERS

Since the entire sensitive volume should be accessible to the charged particles and the width of the "dead layer" should be minimal, the n-p (or p-n) junction must be produced near the surface of the crystal. This is realized by two principal methods.

The first method consists of surface diffusion of matter with additional impurity of one type inside the crystal which has a weak concentration of impurities of the other type [15-17].

In the second method an artificial surface barrier is produced by using the chemical properties of the surface in pure n-silicon or n-germanium [14,18,19].

It must be noted that the carrier mobility is higher in germanium than in silicon and the average energy needed to produce one pair is lower in germanium than in silicon, but the noise level is so high that germanium detectors are used successfully only at low temperatures, usually at liquid-nitrogen temperature [14,19,20]. Silicon detectors are therefore more used in practice.

Counters with diffusion junctions, obtained by diffusion of phosphorus in p-silicon crystals, were successfully used by many workers. The phosphorus can diffuse either from the gaseous state or from the solid one. In the latter case P_2O_5 is deposited directly on the surface of a silicon block, and the latter is placed in a furnace. The depth of penetration of the impurity can be regulated by the temperature at which the diffusion process is carried out, and by the duration of the process.

If the main body of the counter is n-type material and it is necessary to cover it with a p-type coating, the procedure can be analogous. However, in this case it is preferable, in view of the greater simplicity of manufacture, to produce the p-type surface layer not by thermal diffusion of the chemical impurities, but by using the chemical properties of the surface of Si or Ge itself.

The surface of Si or Ge oxidizes readily and behaves like an electron acceptor (p-layer). Electric contact with the surface layer (the inversion region) is by means of a thin layer of metal (usually gold), which is deposited over the semiconductor surface by evaporation in vacuum. The reverse bias applied to the counter increases the thickness of the depletion layer to a considerable depth, as much as a millimeter.

The procedure for the manufacture of silicon counters with gold coating is so simple that it can be effected in any physical laboratory. It is merely necessary to have single crystals of n-type silicon of high purity. The technology for producing such counters can be based on a procedure described in [18].

n-type silicon single crystals, with resistivity 140 ohm-cm, are cut by a diamond disc saw into plates measuring 5×5×1 mm or 2×2×1 mm in such a way

that the larger side corresponds to the crystallographic orientation (111) or, in other words, that the larger side of the plates is perpendicular to the direction of crystal growth. This is followed by the following operations.

1. The specimen is given a mirror finish on a silk-covered rotating wheel, using fine silicon carbide powder as the abrasive.

2. The crystal is washed in pure water and then boiled for ten minutes in concentrated nitric acid.

3. Etching in the following mixture of acids: two parts of concentrated (90%) nitric acid, one part of glacial acetic acid, one part of 40% hydrofluoric acid. The volume of the etchant is 20 cc per crystal.

The mixture is cooled to the temperature of melting ice. The etching is for ten minutes with continuous mixing of the solution to eliminate bubbles produced on the crystal.

4. The sample is washed by successively diluting the etchant with distilled water. The dilute solution is poured off without allowing contact between the crystals and the air. Bidistillate is used during the last stages of washing.

5. The washed crystal is dried with filter paper and transferred to a drying oven (100°C).

6. Metal foil 100 micron thick is glued to two sides of the crystals with BF-2 adhesive. The copper foils extend 1 mm over the crystal. The adhesive is polymerized in the drying oven.

7. The crystal with the copper foils glued to it is clamped between two mica plates, one with a rectangular aperture.

8. A layer of gold is deposited on the crystal and foil through the opening in the mica plate. The sputtering is in vacuum at a pressure of 10^{-5} mm Hg.

To monitor the thickness of the sputtered gold layer, a plate with a copper contact is placed alongside the crystal, and serves to measure the resistance of the sputtered gold layer. The thickness of the layer, which should be 20—40 $\mu g/cm^2$, is determined from the value of the resistance.

9. Gold is sputtered on the opposite side of the crystal in exactly the same way as on the first.

10. After sputtering the gold, the energy resolution is measured by bombarding the crystal with alpha particles of known energy, and the maximum bias that the detector can withstand without breakdown is determined. As a result of these measurements, the best of the two prepared sides of the crystal is chosen to be the working surface.

11. The finished detector is encased in a plastic mount. The adhesive used is usually BF-2, polymerized in a drying oven.

The main advantages of counters with surface barriers is that they are simple to manufacture.

The thickness of the gold film can be easily made homogeneous, and the input window of the surface-barrier counter can be readily made very thin, where-

as counters with diffusion junctions call for very careful control of the surface diffusion, in order to obtain a counter with a thin window.

Volume leakage current is smaller in surface-barrier counters, particularly in counters with large counter area (Au-Ge counters are made with areas up to 6 cm^2, while Au-Si counters are made with areas up to 3 cm^2 [19]).

The simplicity of the evaporation method permits the production of counters of different constructions for special problems:

1. Detectors for the analysis of fission fragments, described in [19]. A thin layer of fissioning material, for example oxide of U^{235}, is deposited by evaporation in vacuum on a layer of gold. Two such counters are placed at a short distance from each other, and the coincidences corresponding to the gathering of both fragments are registered. The use of solid counters makes it possible to dispense with a special substrate for the thin film of fissioning matter, necessary when working with an ionization chamber.

2. Thin dE/dx counters, described in Sec. 6.

3. Neutron detectors, described in Sec. 7.

The main advantage of counters with diffusion junctions is that the presently available material for their manufacture has a much larger resistivity than the material used for surface-barrier p-n counters, thus extending the possibility of using n-p junctions for weakly ionizing radiation and for high-energy heavy particles. These capabilities are expanded even more when the so-called nIp structure is used[21]. The nIp structure is a plate made of high resistance silicon— the I layer—on opposite sides of which thin n- and p-layers are produced by diffusion (Fig. 8). If the bias applied is sufficiently large, the space-charge region extends over the entire I layer. The alpha particles arrive parallel to the junction plane, unlike in the preceding types of counters. As a result, a deeper penetration of the particles in the counters is possible without their going beyond the depletion layer.

An exceptionally valuable variant of the nIp structure are the lithium-silicon detectors manufactured by the compensation method developed by Pell[22]. The technology of their manufacture reduces to the following operations:
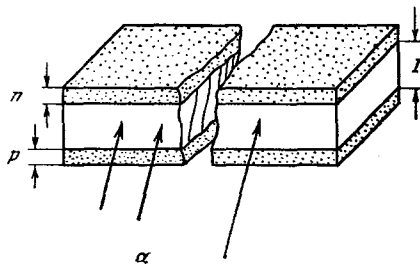

FIG. 8. nIp structure for sufficiently large bias voltage, when the space-charge region extends over the entire I layer. The alpha particles are incident parallel to the junction plane.

1. Produce a thin layer of phosphors in p-type silicon by diffusion.

2. Evaporate a carefully controlled layer of lithium on the top of a layer of phosphorus.

3. Place a thin aluminum plate on the lithium layer.

4. Diffuse the lithium at 400°C through the silicon.

5. Apply a reverse bias of several hundred volts and heat the diode to 150°C. The electric field then causes the lithium ions (intermediate donors of the n-type) to drift deeper inside the p-silicon and compensate for the positive p-type acceptor ions.

The result is a substance with compensated impurity density, which has in practice only the thermally generated carrier density. The maximum attainable resistivity in this method is equal to the intrinsic resistivity of pure silicon at room temperature, $\rho \approx 250,000$ ohm-cm. There are other variants of this technology[23]. These detectors display very valuable properties for the registration of electrons, gamma quanta, and mixed radiation from radioactive isotopes.

The advantages of this type of detectors are:

1. The detectors are made of low-resistivity silicon.

2. The depth of the depletion layer, corresponding to the compensation region, is sufficiently large—up to 6 mm in a detector in the form of a cube 1 cm on the side[24].

The capacitance of counters having a large depletion-layer depth is very low (2—10 pF). They can be made with sufficiently large counting areas (1 cm^2 and more), so that the sensitivity of such counters is high.

4. The manufacturing technology is simple.

5. The counters have good operating stability and retain constant parameters when stored.

3. HEAVY-CHARGED-PARTICLE SPECTROMETERS WITH SEMICONDUCTOR COUNTERS

To obtain the apparatus charged-particle spectrum with the aid of semiconductor counters, it is necessary to amplify and then analyze by amplitudes the pulses produced by the passage of the charged particles; in other words, it is necessary to obtain their amplitude distributions. This is realized with the aid of an electronic circuit consisting of a preamplifier, amplifier with low noise level, and a pulse-height analyzer, preferably of the multichannel type. If a type AI-100 analyzer is used[25], an expander must be added.

The output voltage depends on the detector capacitance and consequently, for different counters and for the same collected charge, the output voltage will be different; this is not convenient. Therefore many authors recommend the use of a preamplifier and amplifier sensitive to charge [26-29]. Circuits of a charge preamplifier and amplifier are given, for example, in [29].

1. Principal Spectrometer Characteristics

The resolution of a spectrometer is determined by the statistical processes of production of electron-

hole pairs. The statistical scatter of the number of produced pairs is determined by their number (the mean-square deviation is $\sim \sqrt{N}$) and depends on the particle energy, the average energy consumed in pair production, and the efficiency with which the carriers are collected. As can be seen from Fig. 9, the collection efficiency of carriers is a function of the bias voltage applied to the junction. It is close to 100% if the ranges of all the particles of the investigated energies fit within the limits of the sensitive volume. The upper limit of the applied voltage is limited by the intrinsic noise level.

Figure 10 shows the influence of the bias voltage on the resolution. The abscissas are the channel numbers and the ordinates the counting rates in the corresponding channels, with the bias voltage as a parameter. The amplitude distributions are given for alpha particles from Cm^{244} and Cm^{242} [18].
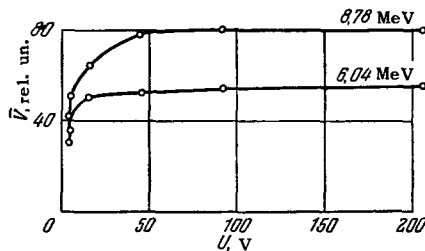

FIG. 9. Efficiency of collection of carriers as a function of the bias voltage for two alpha particles with different energies.
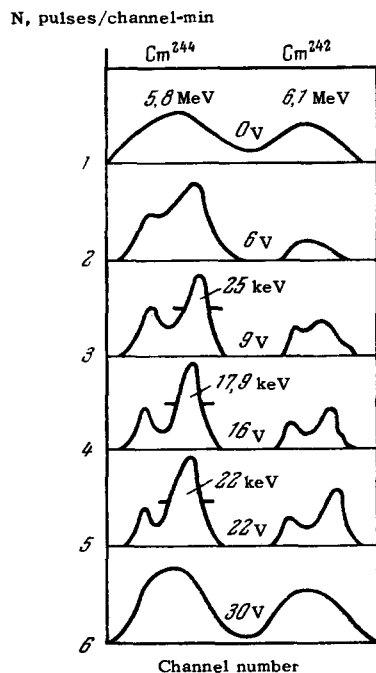
N, pulses/channel-min

FIG. 10. Dependence of the resolution of a spectrometer with semiconductor counters on the bias voltage. 1—U = 0; 2—U = 6 V; 3—U = 9 V, d = 25 keV (6.1 keV/channel); 4—U = 16 V, d = 17.9 keV (15.6 keV/channel); 5—U = 22 V, d = 22 keV (5.9 keV/channel); 6—U = 30 V.

In the case of zero bias, the alpha particles of both isotopes penetrate beyond the limits of the depletion region and therefore the resolution is unsatisfactory. At a bias voltage U = 6 V, the 5.8-MeV alpha particles from Cm^{244} lose essentially their entire energy inside the depletion region, and the fine-structure details can be resolved, whereas for the alpha particles from Cm^{242}, with energy 6.1 MeV, these details do not appear as yet. With further increase in voltage, the resolution (determined, as usual, by the width of the peak at half its height) improves and the fine structure is observed for the alpha particles of Cm^{242}. The best resolution in this example is d = 0.3% and is observed for alpha particles of Cm^{244} at the optimal value U = 16 V. Further increase in the bias voltage leads to an increase in the inverse current and to an increase in the intrinsic noise of the counters, so that the resolution worsens again.

As was already indicated, a rise in the bias voltage decreases, on the other hand, the junction capacitance and increases, on the other hand, the amplitude of the useful signal. The competition between these two effects makes it possible to obtain a sufficiently broad operating range without deterioration of the instrument parameters.

The resolution obtained for alpha particles with energy 5.5 MeV reaches d = 0.3% at a junction area 25 mm^2 [19]*. A resolution d = 0.7% was obtained in [20] for 3-MeV protons.

The range of measured energies for heavy particles is quite broad[20]: up to 50 MeV for alpha particles, 25 MeV for deuterons, and 12 MeV for protons. The lower threshold is determined by the intrinsic noise and its order of magnitude is 20—30 keV.

It must be borne in mind that these data, which pertain to the range of measured energies, have been obtained experimentally and do not represent by any means the limit. With respect to improving the range of measured energies, nIp detectors are particularly promising; it is possible to measure with their aid, as shown in [21], energies of alpha particles up to 100 MeV at an efficient solid angle $\Omega = 2.5 \times 10^{-2}$ sr with 100% collection of the carriers. The detector registration efficiency is $\epsilon = 100\%$.

Lithium-silicon detectors with a compensation-layer depth $l = 6$ mm make it possible to broaden the range of measured energies for heavy particles even more. This counter can be used to investigate the particles having a range of 1 cm in silicon, corresponding to an energy range of up to 190 MeV for alpha particles, 50 MeV for protons, and 5 MeV for electrons.

Most investigations of the nuclear structure lie in this energy range. The resolution obtained for 42.7-MeV alpha particles was found to be d = 0.2% [24].

*The time resolution of surface-barrier detectors was measured by I. V. Baranov and was found to be $\sim 5 \times 10^{-9}$ sec.[39]

2. Background due to Extraneous Radiation

In view of the relatively low atomic number of silicon, it is an almost pure Compton scatterer of gamma radiation. The recoil electrons produced in thin barriers give up only a small fraction of their energy. As a result, the gamma rays produce pulses of very low amplitude at the detector output. It is possible to get rid of the large backgound of such low-amplitude pulses by regulating the depth of the barrier, and also by using a small load resistance and amplifiers with small time constants[19,30,31].

Neutrons can produce pulses in detectors with surface barriers by three possible means: excitation of nuclear reactions in silicon, excitation of nuclear reactions in the gold coating, and formation of recoil protons by elastic scattering of the neutrons in hydrogen-containing impurities (moisture film on the detector). From among the nuclear reactions excited by neutrons in Si, the most important is

$$Si^{28}(n, p): Q = 3.86 \text{ MeV}$$
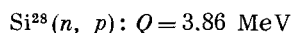
The relative probability of a reaction of this type is 92%.

The effective cross section increases from $\sigma = 0.02$b at $E_n = 5$ MeV to $\sigma = 0.40$b at $E_n = 8$ MeV, and again decreases to $\sigma = 0.22$b at $E_n = 14$ MeV.

We recall also the $Si^{28}(n, \gamma)$ reaction with $Q = -2.66$ MeV. The relative probability of a reaction of this type is 4.7%; $\sigma = 0.1$b at $E_n = 14$ MeV and is practically the same as in the fundamental reaction at $E_n = 6.3$ MeV, that is, of the order of $\sigma = 0.3$b.

Owing to the large atomic number of gold, only neutron capture with emission of gamma rays of energy $E_\gamma = 412$ keV is possible in the gold layer. However, the intensity of this radiation is extremely small for gold films 50 μg/cm^2 thick. Neutrons may knock out recoil protons from the absorbed hydrogen and water vapor on the surface of the detector and in the neighboring surfaces. These protons will be registered by the detector. It is therefore necessary to take measures against possible contamination of the detector with hydrogen-containing substances (all parts must be heated in vacuum and stored in a dry place).

Thus, the most important reactions in the production of a background due to fast neutrons are $Si^{28}(n, p)$ and $Si^{28}(n, \gamma)$, which impose a certain limitation on the use of silicon detectors of any type in a fast-neutron flux, particularly at energies near 8 MeV. However, as in the case of the gamma-radiation background, the sensitivity of the detectors to the neutrons can be reduced to a minimum by regulating the depth of the barrier. In addition, inasmuch as the reactions with silicon and their cross sections are known, they can be taken into account in the reduction of the spectra.

All semiconductor detectors are sensitive to visible light and have photoconductivity, so that they must be placed in light-tight containers.

The counters are not sensitive to magnetic fields. In accordance with [19] and [24], no noticeable effect should be observed in silicon if the field is weaker than 50,000 Gauss.

4. USE OF SEMICONDUCTOR DETECTORS FOR THE REGISTRATION AND SPECTROMETRY OF ELECTRONS

On the basis of an analysis of the physical processes in semiconductors occurring under the action of charged particles, one can expect the amplitude of the pulses produced by electrons to be much smaller, and the resolution much poorer, than for excitation with heavy charged particles. It is therefore understandable why the registration and spectrometry of electrons with the aid of semiconductor counters and spectrometers has received little attention until recently.

It is noted in [26] that the peaks of the conversion electrons from Co^{57} with energies 115 and 121 keV are well resolved; the same reference reports a sufficiently detailed investigation of a semiconductor detector 3 mm in diameter with a very thin window, made by diffusion of phosphorus on a base of p-silicon with resistivity 12000 ohm-cm.

From [26] we can conclude that semiconductor detectors with thin barriers are less promising for the registration and spectrometry of electrons than for heavy particles, owing to the low resolution, small signal amplitude, and narrow range of measured energies.

Further development of spectrometry of electrons with the aid of semiconductor detectors has followed two principal directions:

1. Development of thick surface-barrier detectors with guard ring[24,34].

2. Development of lithium-silicon detectors[23,24].

Borkowski and Fox[35] have shown that the bias voltage $U_{max} = 200$ V, which is assumed to be the maximum at room temperature, is by far not the limit. It can be greatly increased by improving the technology of manufacture of surface-barrier counters (elimination of convexities, sharp edges, introduction of protective electrodes) and can be raised to $U_{max} = 4000$ V with a depletion layer several millimeters deep. Such detectors were used by the authors at room temperature to obtain a resolution d = 1.5% for 0.976-MeV conversion electrons from Bi^{207}.

It is possible to trace on Fig. 11 the influence of cooling of the detector on the quality of the resolution and on the reduction of the background. At room temperature there appear the K and L peaks of the conversion electrons (Fig. 11a), at 0°C the conversion line of the M shell appears (Fig. 11b), and at the temperature of liquid nitrogen the fine structure of the L line appears (Fig. 11c).

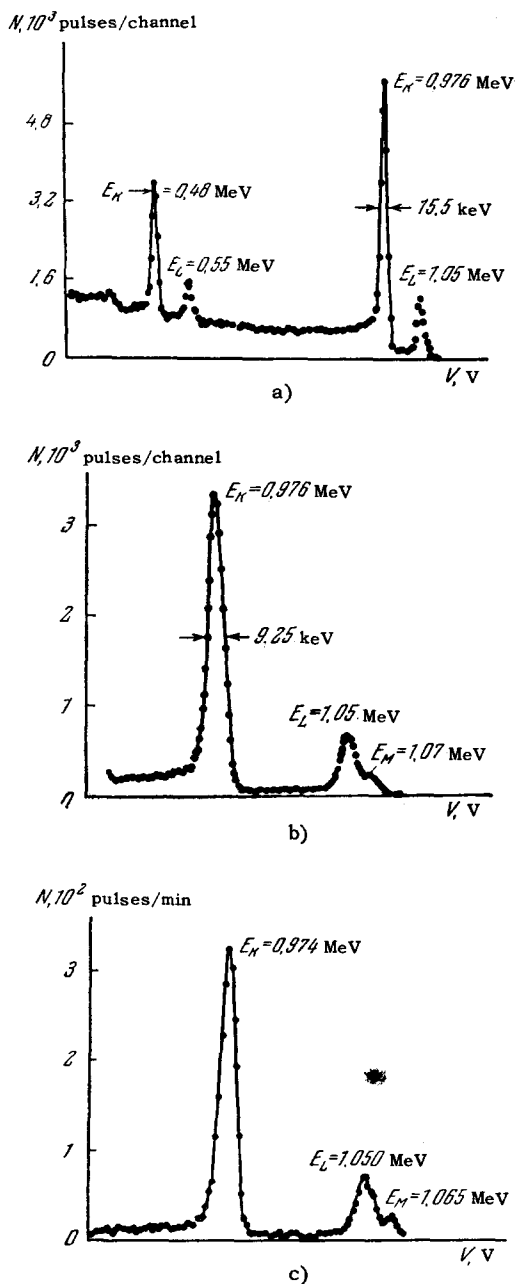When the depletion layer depth is several millimeters, the characteristics of the lithium drift silicon

$N, 10^3$ pulses/channel

$E_K = 0.976$ MeV

4.8

3.2　　$E_K \rightarrow = 0.48$ MeV

15.5 keV

$E_L = 0.55$ MeV　　　　$E_L = 1.05$ MeV

1.6

0

V, V

a)

$N, 10^3$ pulses/channel

$E_K = 0.976$ MeV

3

9.25 keV

2

$E_L = 1.05$ MeV

1　　　　　　　　$E_M = 1.07$ MeV

0

V, V

b)

$N, 10^2$ pulses/min

$E_K = 0.974$ MeV

3

2

$E_L = 1.050$ MeV

1　　　　　　　$E_M = 1.065$ MeV

0

V, V

c)

FIG. 11. Spectrum of internal-conversion electrons of Bi^{207}, obtained with a surface-barrier detector and guard electrode (detector area 20 mm^2, ρ = 6000 ohm-cm). a)Temperature t = 22°C, U = 1800 V; b) temperature t = 0°C, U = 1200 V; c) temperature of liquid nitrogen, U = 200 V; detector area 25 mm^2.

counters are close to those of the described surface-barrier counters. In both cases it is possible to obtain almost windowless detectors (dead layer < 100 μg/cm^2).

5. USE OF SEMICONDUCTOR DETECTORS FOR THE REGISTRATION AND SPECTROMETRY OF GAMMA RADIATION

Inasmuch as the energy spectrum of gamma radiation is determined by spectrometers with semiconduc-

tor detectors indirectly, by measuring the energy of secondary electrons produced by the gamma quanta in the detector material (photoelectrons, Compton recoil electrons, electron-positron pairs), detectors with thin barriers are of little use for this purpose. Better results can be obtained with detectors with nIp structure, described in [21].

Spectra of Hg^{203} and Cs^{137} are given in that reference. The resolution obtained for the gamma radiation from Hg^{203} (E_γ = 279 keV) was d = 8% (from the photopeak).

From the obtained value of the maximum pulse amplitude corresponding to the photoelectrons, the average energy lost by an electron and consumed in the production of one pair (electron plus hole) was calculated to be

$$\bar{\mathscr{E}} = 3.53 \pm 0.07 \text{ eV in the case of } Hg^{203}$$

and

$$\bar{\mathscr{E}} = 3.55 \pm 0.07 \text{ eV in the case of } Cs^{137}.$$

This value corresponds to the previously published value of the mean energy used to produce an electron-hole pair in silicon, for alpha particles and protons, namely

$$\bar{\mathscr{E}}_\alpha = \bar{\mathscr{E}}_p = 3.50 \pm 0.05 \text{ eV}.$$

A suggestion is made in [21] that actually the greater part of the electron-hole pairs are produced on passage of heavy charge particles through a crystal is due to δ-electrons with energy of several keV.

Very good results were obtained with lithium-silicon detectors. It is possible to determine with their aid the energy of gamma quanta both from the photoabsorption peaks in silicon and from the clearly pronounced edges of the Compton distributions of the recoil electrons. Gamma spectra were obtained for Cr^{51}, I^{131}, Cs^{137}, and Co^{60}. The resolution obtained for Cs^{137} from the photopeak was d = 1.5%, which is higher than the resolution obtained with scintillation counters [23,24].

6. THIN dE/dx COUNTERS

Semiconductors were used essentially to measure energies of particles with relatively low energies and with ranges smaller than the width of the depletion layer. In addition to using the nIp structure, there is another way of increasing the range of measured energies, consisting of using semiconductor detectors as dE/dx counters [19,27].

dE/dx counters make use of the experimental fact that the relation between the energy lost per unit path length dE/dx and the particle energy has a clearly pronounced minimum.

In silicon dE/dx counters, the energy loss at minimum ionization, for any particle with low ionization density, is of the order of 400 keV/mm. This raises

difficulties in itself. Inasmuch as the detector operates in the region of minimum ionization, the pulse amplitudes are small and need appreciable amplification, while the amplitude scatter of the pulses, due to the statistical fluctuations, reaches ~ 20% and more.

7. USE OF SEMICONDUCTOR DETECTORS FOR NEUTRON SPECTROMETRY

Surface-barrier silicon counters were used for the registration and spectrometry of both fast and slow neutrons. Two main counter constructions were developed for this purpose.

In one construction use is made of the nuclear re-

action $Li^6(n, \alpha)T$. A thin layer of Li^6F is deposited by sputtering in vacuum on the surface of one of the Au-Si counters[32,20]. At a small distance from this counter (0.05 mm) there is fastened a second Au-Si counter, analogous to the first. The construction of the dual "sandwich" counter is shown in Fig. 12. The neutrons are detected by observation of (α + T) pairs. The pulses from the two counters are summed and the summary pulse amplified and recorded with a multichannel analyzer. The amplitude of the summary pulse is proportional to the neutron energy plus the reaction energy (E_n + Q), as can be seen from Fig. 13.
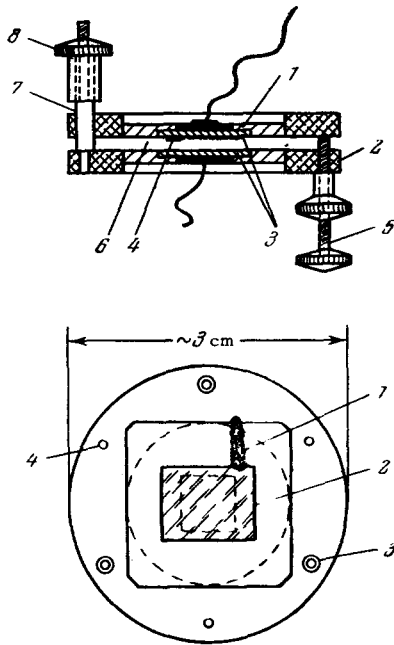

FIG. 12. Fast neutron detector with Li^6F layer. 1—Si; 2—Al; 3—Au; 4—Li^6F; 5—setting screw; 6—air gap, 0.01 mm; 7—guide rod; 8—lock nut.
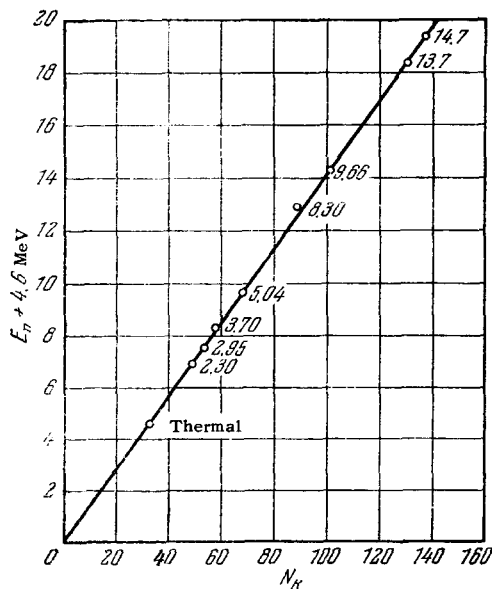

FIG. 14. Slow-neutron spectrum. 1—Main peak, 2—single-particle peak.

FIG. 13. Dependence of pulse amplitude on the neutron energy.
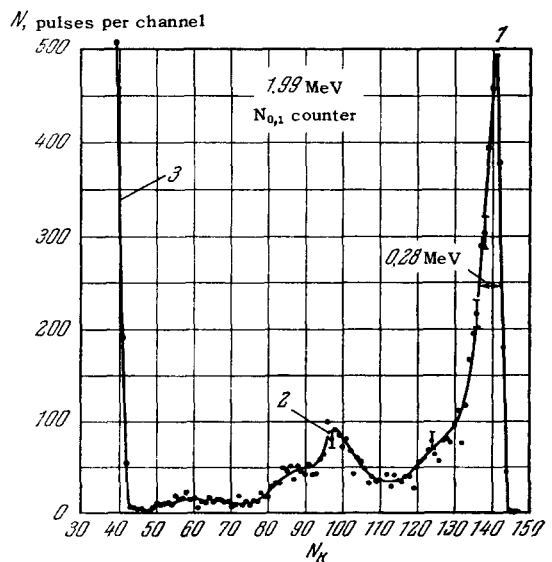

FIG. 15. Spectrum of monoenergetic neutrons with energy 1.99 MeV. 1—Main peak, 2—slow-neutron peak, 3—recoil-proton peak.

Examples of the recorded amplitude distributions produced by slow and monoenergetic fast neutrons with energies 1.99 and 14 MeV are shown in Figs. 14, 15, and 16 respectively.

Figure 14 shows the spectrum of slow neutrons, obtained by moderating fast neutrons from a Po-Be source in paraffin, or from the reaction $T(p, n)He^3$ in a Van de Graaff generator. To the left of the slow-neutron peak there is observed a "single-particle peak" obtained as a result of registration of tritons only (edge effect). The peak from the alpha particles only is not observed, owing to the large energy lost when the alpha particles pass through the layer of gold and the Li^6F [20]. The edge effect can be eliminated by sputtering the Li^6F on an area smaller than the total counter area of the detector.
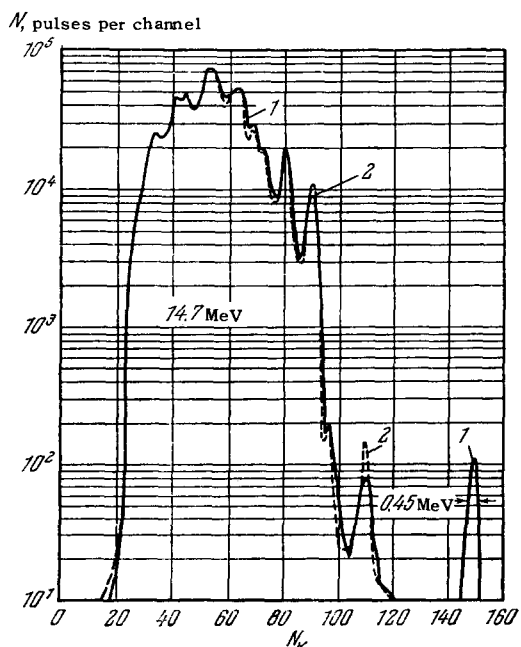

FIG. 16. Spectrum of neutrons with energy 14.7 MeV, obtained from the reaction $T(d, n)He^4$. Solid curve—obtained with a surface-barrier counter with Li^6F layer; dashed curve—without layer.

Figure 15 shows the peak of the slow neutrons (2) in addition to the main peak (1); the single-particle peak is not noticeable, and the recoil proton distribution (3) appears on the left. Figure 16 gives the spectrum of fast 14.7-MeV neutrons, obtained from the reaction $T(d, n)Ag^4$. The solid curve is obtained with the aid of a counter containing Li^6F, and the dashed curve with a counter without such a layer. It is clearly seen from the figure that the background is due to the reactions in silicon and gold, but not in Li^6F.

The counter efficiency is limited and depends on the reaction cross section and the thickness of the Li^6F. With an Li^6F layer 150 $\mu g/cm^2$ thick, the efficiency for thermal neutrons is $\epsilon_T = 3 \times 10^{-3}$, and for fast

neutrons with energy 2 MeV it is $\epsilon = 1 \times 10^{-6}$ (with normal incidence of the neutron beam on the counter). The resolution depends little on the neutron energy.

The second type of construction is shown in Fig. 17 [19]. The counter operates by the recoil-nucleus method. It consists of a silicon disc Si, on which two half-round gold layers are deposited by evaporation in vacuum (through a mask). Contacts A and B are secured in the usual manner. Both halves and both counters should give identical readings when plotting the spectrum of the background pulses.

A scatterer layer (glycerol tristearate or polyethylene-R) is then deposited on the gold layer of one of the counters and serves as a source of recoil protons when the counter is bombarded with fast neutrons.

If the counters are connected in a subtraction circuit, the net recoil-proton spectrum from the scatterer is obtained.

Figure 18 shows the spectrum of the recoil protons, obtained with the aid of this method. The counters were bombarded with monoenergetic neutrons with energy 3.7 MeV. The neutron spectrom was obtained, as usual, by differentiating the obtained amplitude distribution of the recoil protons.

When large neutron fluxes are measured, the efficiency does not play a major role. The principal role is assumed here by the possibility of loading the detector with large neutron fluxes without damage.

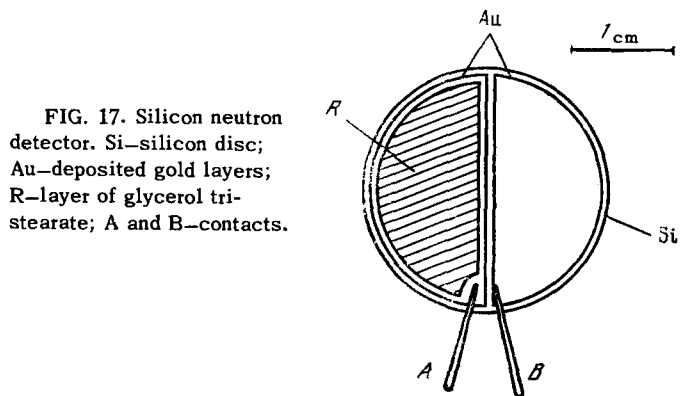This question was investigated in [37] and [38]. The

FIG. 17. Silicon neutron detector. Si—silicon disc; Au—deposited gold layers; R—layer of glycerol tristearate; A and B—contacts.
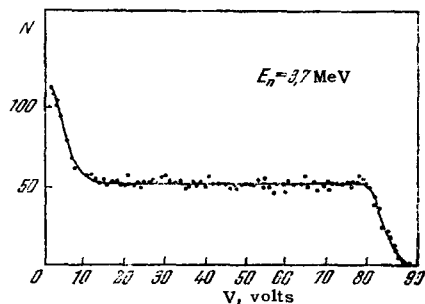

FIG. 18. Spectrum of recoil protons, obtained using the counter shown in Fig. 17, from a monoenergetic beam of neutrons with energy $E_n = 3.7$ MeV.

results of the investigations of [38] are shown in Figs.
19 and 20. It is seen from these figures that semicon-
ductor detectors are sufficiently stable, and also that
from the variation of the inverse current and the form
of the spectrum it is possible to measure quite large
doses of fast neutrons.

Unfortunately, it is not quite clear how reversible
the damage produced by large doses of fast neutrons
is. It is possible that at large doses, 10^4 rad and more,
the instrument can be used only once.

8. FIELDS OF APPLICATION OF SPECTROMETERS WITH SEMICONDUCTOR DETECTORS

The most important field of application of spec-
trometers with semiconductor detectors is the spec-
trometry of heavy charged particles and fission frag-
ments.

1) α-spectrometry. A sufficiently extensive use of
spectrometers with semiconductor detectors should re-

sult in a very rapid progress in alpha spectrometry.
Until recently this field of spectrometry has been very
slow in developing, because the ionization and scintil-
lation methods of alpha spectrometry have relatively
low resolution. On the other hand, magnetic alpha
spectrometers, although possessing good resolution,
are exceedingly expensive, cumbersome, and call for
stable magnetic fields on the order of tens of thousands
of Gauss; the plotting of a spectrum with magnetic
alpha spectrometers is a very laborious process.

2) Spectrometry of the products of nuclear reac-
tions on accelerator targets. Spectrometers with
semiconductor detectors make it possible to observe
the entire spectrum simultaneously. The linear energy
dependence of the instrument sensitivity facilitates the
calibration of the spectrometer and simplifies the in-
terpretation of the spectrum. The small transmitter
dimensions make it possible to move it readily around
the target through angles approaching 180° (something
which usually cannot be done with the magnetic instru-
ment), and new experimental data can be obtained for
such angles.

By way of an example, Fig. 21 shows the spectrum
obtained as a result of bombarding a thin target con-
taining carbon, boron, and oxygen with deuterons having
an energy $E_d = 5$ MeV.

3) Separation and identification of different particles
by their ranges. This is carried on by varying and con-
trolling the width of the sensitive layer l, and in this
case the control bias U can be changed remotely. It
must be noted that the variation of the control bias has
a smaller effect on resolution than the previously em-
ployed decelerating foils. In addition, owing to the sta-
bility against overload ($\sim 10^{14}$ protons/cm^2), semicon-
ductor detectors can be successfully used to monitor
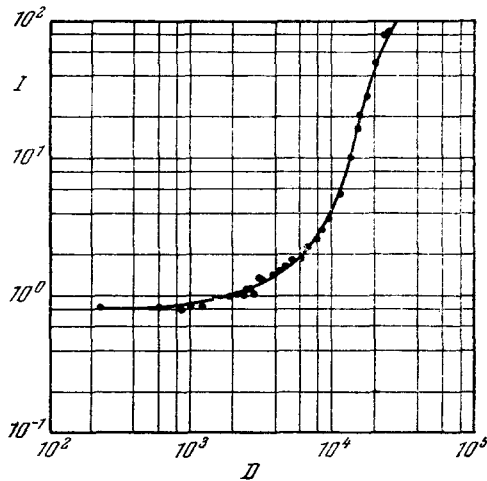proton and deuteron beams in accelerators.

FIG. 19. Dependence of the inverse current on the integral
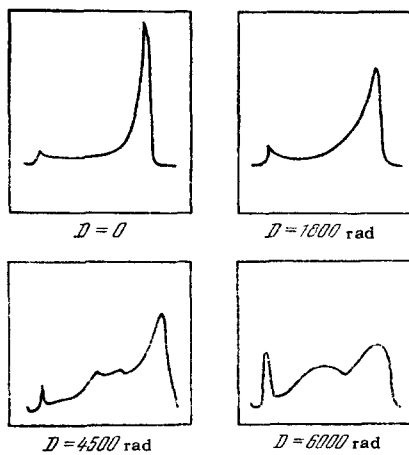dose of fast neutrons for gold-silicon detector.

FIG. 20. Variation of the spectrum of alpha particles of Pu^{239},
obtained with a gold-silicon detector as a function of the fast-
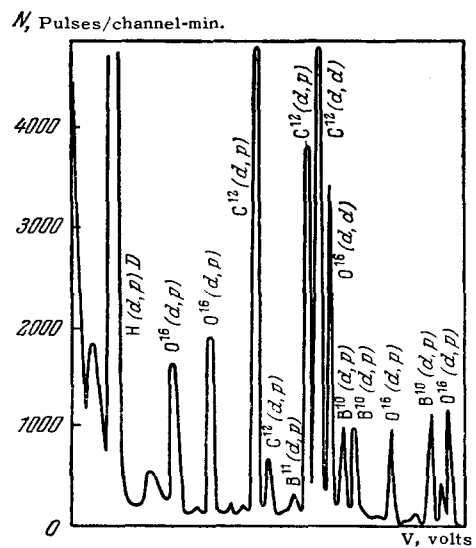neutron dose. The dose (in rad) is indicated on the figure.

FIG. 21. Spectrum obtained with the aid of a surface-barrier
silicon counter with gold coating from a thin target containing
carbon, boron, and oxygen.

4) Measurement of neutron spectra in the presence of gamma background. Because semiconductor detectors can withstand considerable neutron fluxes (up to 10 fast neutrons per cm^2 and more)[37,38,39,42,43], they may turn out to be exceedingly useful in the measurement of fast-neutron fluxes and energies in the active zones of low-power reactors, and when neutrons seep through slots and openings in reactor shields[40]. Heretofore these problems were solved essentially by calculation[41], since the possible experiments with the aid of threshold detectors yielded only crude estimates of the fluxes and particularly of the fast-neutron spectra.

Silicon-carbon fission detectors are proposed for this purpose in [44], where it is indicated that these detectors are capable of withstanding the highest temperatures of reactor coolants and are much more stable against radiation damage than silicon fission counters.

5) Investigation of fission processes. The absence of a dead layer, of an input window, and of a dependence of the results on the specific ionization makes it possible to employ semiconductor counters to investigate fission processes.

Surface-barrier semiconductor detectors were coated with a layer of investigated fissioning matter (U^{235}, U^{233}, Pu^{239}) and were inserted as a unit together with a transistorized preamplifier, for several hours inside a thermal column, where the thermal neutron flux was $\sim 10^9$ thermal neutrons/cm^2 sec. The output was connected to an analyzer to measure the energy of the fission fragments. The authors note that the high statistical measurement accuracy yielded the fine structure of the fission, and that this has led to new ideas concerning the fission mechanism[24].

6) Experiments in outer space. Owing to the small dimensions and weights and owing to the use of low-voltage power supplies and weak sensitivity to fields, semiconductor detectors are indispensable for experiments in outer space (for the analysis of the composition and energy of cosmic rays, for the determination of the radiation belts, for investigation of flares on the sun, etc.).

Many systems have already been constructed for such experiments. There are also combined systems; for example, the cosmic-ray telescope described in [45] is a combination of semiconductor detectors and scintillation counters.

CONCLUSION

Spectrometers for heavy charged particles with semiconductor detectors have many valuable properties.

Because the charged particles (protons, alpha particles, heavy ions) are decelerated in a thin layer of matter, on the order of several hundred microns, it is possible to produce in this layer an electric field of $\sim 10^4$ V/cm with the aid of a small bias voltage— several hundred volts or less. Consequently, the pulses produced in the transducer have a steep front ($\sim 10^{-9}$ sec). The energy consumed in the production of one pair of charges in a semiconductor detector is one-tenth the average energy used in a gas ionization chamber, so that more ion pairs are produced in the detector, and all of their charge can be collected; this ensures good resolution, on the order of several tenths of one per cent. Large pulses due to heavy particles, with very small effect of gamma radiation on the semiconductor detector, make it possible to register heavy charged particles in the presence of a considerable gamma-ray background.

The linearity of semiconductor detectors over a wide energy range (from several times 10 keV to 100 MeV and more for alpha particles) ensures a sufficiently broad range of measured energies, simplifies the spectrometer calibration and the interpretation of the spectra.

Semiconductor spectrometers are compact, cheap, and simple to manufacture and use. They are useful under complicated experimental conditions at low temperatures, in vacuum, and in strong magnetic fields. There is no doubt that in the near future spectrometers with semiconductor detectors will be most extensively used in the spectrometry of heavy charged particles and fission fragments. They can be employed in the spectrometry of low-energy electrons, soft x-rays and gamma rays, and also in neutron spectrometry.

The main shortcoming of spectrometers with semiconductor detectors is their low geometrical efficiency, due to the small dimensions of the detectors, so that when the detector registration is 100% efficient the source utilization coefficient is very low.

Because a large counter area leads to a deterioration of the detector resolution, many authors have attempted to employ mosaics. Greenberg used 32 elements connected in parallel and forming a mosaic, and employed this system for the analysis of heavy ions in research on Coulomb excitation. The over-all resolution of the system which he obtained was 6%.

Steinberg used a system of 10 series-connected detectors for the analysis of neutron fluxes.

Discrete mosaics with individual registration units were employed in measurements based on analysis of angular distribution of charged particles, and also in the focal plane of a magnetic spectrometer as a dynamic substitute for photographic film.

[1] Golovin, Osipenko, and Sidorov, PTÉ, No. 6, 5 (1961).

[2] K. A. Jamakawa, Phys. Rev. 75, 1774 (1949).

[3] H. Kallman and R. Warminsky, Ann. Phys. 4, 69 (1948).

[4] G. J. Goldsmith and K. Lark-Horovitz, Phys. Rev. 75, 526 (1949).

[5] S. M. Ryvkin, ZhTF 26, 2667 (1956), Soviet Phys. Tech. Phys. 1, 2580 (1957).

[6] I. P. Stepanovich, Principles of Transistor Engineering (offset edition), Moscow Eng. Phys. Inst., 1958. M. J. O. Strutt, Transistoren, S. Hirzel, Leipzig, 1954.

[7] A. C. Prior, J. Chem. Phys. Solids 12, 175 (1960).

[8] G. A. Tyagunov, Elektrovakuumnye i poluprovodnikovye pribory (Vacuum Tubes and Transistors), Gosenergoizdat, 1962.

[9] W. L. Brown, IRE Trans. Nucl. Sci. 8(1), 2 (1961).

[10] W. Kaiser and G. H. Wheatley, Phys. Rev. Letts 3, 334 (1959).

[11] C. B. Collins and R. O. Carlson, Phys. Rev. 108, 1409 (1957).

[12] W. D. Davis, Phys. Rev. 114, 1006 (1959).

[13] J. D. Van. Putten and I. C. Van de Velde, Bull. Am. Phys. Soc. 5, 3 (1960).

[14] Walter, Dabbs, and Roberts, Rev. Sci. Instr. 37, 7 (1960).

[15] Ryvkin, Maslova, Matveev, Strokan, and Tarkhin, Atomnaya energiya 11, 217 (1961).

[16] Stefen, Fridland, James, Mayer, John, and Wiggins, Nucleonics 18, 2 (1960).

[17] M. Halbert and J. Blankenship, Nucl. Instr. and Meth. 8(1), 106 (1960).

[18] Bredel', Mikheev, and Polikanov, PTÉ, No. 6, 44 (1961).

[19] G. Dearnaley and A. B. Wheitehead, Nucl. Instr. and Meth. 12(2), 206 (1961).

[20] F. A. Love and R. B. Murray, IRE Trans. Nucl. Sci. 8(1), 91 (1961).

[21] Koch, Messier, and Valin, IRE Trans. Nucl. Sci. 8(1), 43 (1961).

[22] E. M. Pell, J. Appl. Phys. 31, 291 (1960).

[23] N. A. Baily and J. W. Mayer, IRE Trans. Nucl. Sci. 9(1), 91 (1962).

[24] D. Allan Bromley, Nucleonics 20(5), 55 (1962).

[25] A. A. Sanin, Elektronnye pribory v yadernoĭ fizike (Electronic Instruments in Nuclear Physics), Fizmatgiz, 1961.

[26] J. L. Blankenship, C. J. Borkowski, IRE Trans. Nucl. Sci. 8 (1), 17 (1961).

[27] E. Fairstein, IRE Trans. Nucl. Soc. 8 (1), 129 (1961).

[28] Chase, Higinbotam, and Müller, IRE Trans. Nucl. Sci. 8(1), 197 (1961).

[29] Maslova, Matveev, Ryvkin, Strokan, Tarkhin, and Khozov, Izv. AN SSSR ser. fiz. 26, 1498 (1962), Columbia Tech. Transl. p. 1524.

[30] J. M. McKenzie and G. T. Ewans, IRE Trans. Nucl. Sci. 8(1), 50 (1961).

[31] Cottini, Gatti, Grianelli, and Rossi, Nuovo cimento, 473 (1961).

[32] F. A. Love and R. B. Murray, ORNL Report C. F. 60, 5 (1960).

[33] J. M. McKenzie and G. T. Ewans, IRE Trans. Nucl. Sci. 8(1) (1961).

[34] Zubritskiĭ, Chursin, Gonchar, and Zalyubovskiĭ, Surface-barrier Semiconductor Counters with Guard Electrode, Paper at Thirteenth All-union Conference on Nuclear Spectroscopy, Jan. 21—Feb. 2, 1963.

[35] R. J. Fox and C. J. Borkowski, Paper at Eighth Symposium on Scintillation and Semiconductor Counters, March 1962. IRE Trans. Nucl. Sci. 9, 213 (1962).

[36] H. E. Wegner, IRE Trans. Nucl. Sci. 8(1), 103 (1961).

[37] R. V. Babcock, IRE Trans. Nucl. Sci. 8(1), 204 (1961).

[38] R. W. Klingernsmith, IRE Trans. Nucl. Sci. 8(1), 112 (1961).

[39] I. V. Baranov, Measurement of Time Resolution of Semiconductor Detectors, op. cit. [34].

[40] E. L. Stolyarova, Methods of Fast-neutron Spectroscopy and Prospects of Their Use in Neutron Dosimetry. Neutron Dosimetry, v. 2, Intern. Atomic Energy Agency, Vienna, 1963, p. 67.

[41] V. N. Mironov, Atomnaya énergiya 12, 21 (1962)

[42] R. Steinberg, IRE Trans. Nucl. Sci. 9(1), 97 (1962).

[43] R. V. Babcock, Nucleonics 17(4), 116 (1959).

[44] R. V. Babcock and H. C. Chang, SiC Neutron Detectors for High Temperature Operation Symposium on Neutron Detection, Dosimetry and Standardization. Harwell, United Kingdom, 10—14 December 1962.

[45] Report of Eighth Symposium on Scintillation and Semiconductor Counters, Nucleonics 20, 53 (1962).

Translated by J. G. Adashko